(*15*). Intrathymically, stromal cell–associated class II molecules interact with T lymphocyte precursors to establish self tolerance and determine the specificity of the mature T cell repertoire (*19*). In peripheral lymphoid organs, class II molecules bind antigen fragments to form a bimolecular complex, which can then be recognized by the antigen receptor on $CD4^+CD8^-$ T cells (*20*). A variant class II molecule could thus contribute to autoimmune disease susceptibility by influencing T cell repertoire development or by altering antigen-binding properties. The latter possibility could be tested if sufficient quantities of the putative epidermal cell PV autoantigen become available.

REFERENCES AND NOTES

1. A. Svejgaard, P. Platz, L. P. Ryder, *Immunol. Rev.* **70**, 193 (1983).
2. J. F. Kaufman, C. Auffray, A. J. Korman, D. A. Shackelford, J. L. Strominger, *Cell* **36**, 1 (1984).
3. M. Michaelides *et al.*, *J. Exp. Med.* **153**, 464 (1981); C. Lin, A. S. Rosenthal, H. C. Passmore, T. H. Hansen, *Proc. Natl. Acad. Sci. U.S.A.* **78**, 6406 (1981); L. Mengle-Gaw, S. Conner, H. O. McDevitt, C. G. Fathman, *J. Exp. Med.* **160**, 1184 (1984); P. Christadoss, J. M. Lindstrom, R. W. Melvold, N. Talal, *Immunogenetics* **21**, 33 (1985).
4. G. Schreuder *et al.*, *J. Exp. Med.* **164**, 938 (1986); J. Goronzy, C. Weyand, C. G. Fathman, *J. Clin. Invest.* **77**, 1042 (1986); D. Owerbach *et al.*, *Nature (London)* **303**, 815 (1983); O. Cohen-Hagenauer *et al.*, *Proc. Natl. Acad. Sci. U.S.A.* **82**, 3335 (1985).
5. F. Szafer, C. Brautbar, A. Friedmann, E. Tzfoni, L. Steinman, *Proc. Natl. Acad. Sci. U.S.A.* **84**, 6542 (1987).
6. K. H. Singer, K. Hashimoto, P. J. Jensen, S. Morioka, G. S. Lazarus, *Annu. Rev. Immunol.* **3**, 87 (1985); J. R. Stanley, M. Yaar, P. Hawley-Nelson, S. I. Katz, *J. Clin. Invest.* **70**, 281 (1982).
7. A. R. Ahmed, in *Clinics in Dermatology—Pemphigus Vulgaris*, A. R. Ahmed, Ed. (Lippincott, Philadelphia, 1983), p. 13.
8. W. F. Bodmer *et al.*, *Tissue Antigens* **24**, 73 (1984); N. Ishikawa *et al.*, *Immunogenetics* **26**, 143 (1987).
9. R. Duquesnoy, M. Marrari, K. Annen, *Transplant. Proc.* **11**, 1757 (1979).
10. D. A. Shackelford, B. Eibl, J. L. Strominger, *Immunogenetics* **18**, 625 (1983); M. Trucco and R. J. Duquesnoy, *Immunol. Today* **7**, 297 (1986).
11. S. Rosenshine, I. Lascino, A. Zeevi, F. J. Duquesnoy, M. Trucco, *Immunogenetics* **23**, 187 (1986).
12. B. S. M. Lee, J. I. Bell, N. A. Rust, H. O. McDevitt, *ibid.* **26**, 85 (1987).
13. L. Mengle-Gaw and H. O. McDevitt, *Annu. Rev. Immunol.* **3**, 367 (1985).
14. R. K. Saiki *et al.*, *Nature (London)* **324**, 163 (1986).
15. J. A. Todd *et al.*, *ibid.* **329**, 599 (1987).
16. D. Larhammar *et al.*, *Proc. Natl. Acad. Sci. U.S.A.* **80**, 7313 (1983).
17. J. Gorski and B. Mach, *Nature (London)* **322**, 67 (1986).
18. J. Silver and S. M. Goyert, in *HLA Class II Antigens*, B. G. Southern, E. Moller, S. Ferrone, Eds. (Springer-Verlag, Berlin, 1986), p. 32; C. G. Fathman, J. Goronzy, C. Weyand, *Ann. N.Y. Acad. Sci.* **475**, 24 (1986).
19. D. L. Longo, A. M. Kruisbeek, M. L. Davis, L. A. Matis, *Proc. Natl. Acad. Sci. U.S.A.* **82**, 5900 (1985); D. Lo and J. Sprent, *Nature (London)* **319**, 672 (1986); J. W. Kappler, N. Roehm, P. Marrack, *Cell* **49**, 273 (1987).
20. E. R. Unanue and P. M. Allen, *Science* **236**, 551 (1987); J.-G. Guillet *et al.*, *ibid.* **235**, 865 (1987); S. Buus, A. Sette, S. M. Colon, C. Miles, H. M. Grey, *ibid.*, p. 1353.
21. E. Turco *et al.*, *Immunogenetics* **26**, 282 (1987).
22. L. Schenning *et al.*, *EMBO J.* **3**, 447 (1984).
23. J. I. Bell *et al.*, *Proc. Natl. Acad. Sci. U.S.A.* **82**, 3405 (1985).
24. B. Carlsson, J. Wallin, J. Bohme, E. Moler, *Human Immunol.* **20**, 95 (1987).
25. P. K. Gregerson *et al.*, *Proc. Natl. Acad. Sci. U.S.A.* **83**, 2642 (1986).
26. J. I. Bell *et al.*, *J. Immunol.* **139**, 562 (1987).
27. V. Gubler and B. J. Hoffman, *Gene* **25**, 263 (1983).
28. M. M. Y. Waye, M. E. Verhoeyen, P. T. Jones, G. Winter, *Nucleic Acids Res.* **13**, 8561 (1985).

29. A.A.S. is a Centennial fellow of the Medical Research Council of Canada and is a recipient of an independent research allowance from the Alberta Heritage Foundation for Medical Research. J.A.T. gratefully acknowledges fellowships from the European Molecular Biology Organization and the Science and Engineering Research Council. This work was supported by the National Institutes of Health. We thank P. Travers, C. Jacob, and Z. Fronek for helpful discussions and critical review of the manuscript, B. Lee and P. Patek for reagents, M. Trucco for data prior to publication, and K. Karagianes and K. Moody for final preparation of the manuscript.

16 September 1987; accepted 19 January 1988

Atrial Natriuretic Factor–SV40 T Antigen Transgenes Produce Tumors and Cardiac Arrhythmias in Mice

LOREN J. FIELD

Transgenic mice that carry fusions between the transcriptional regulatory sequences of atrial natriuretic factor (a hormone intimately involved in the regulation of blood pressure) and those encoding SV40 T antigen (an oncoprotein) were generated. Although both atria express the fusion gene, the pathological response to T antigen is asymmetrical. The right atrium undergoes a several hundredfold increase in mass while the left atrium remains relatively normal in size. Hyperplasia is accompanied by a progressive increase in both the frequency and severity of abnormalities in the atrial conduction system, which ultimately result in death.

NORMAL HEART FUNCTION IS DEpendent on the coordinated depolarization and contraction of atrial and ventricle myocardiocytes. Abnormalities in this conduction system can impair cardiac function, often with catastrophic effects. Although it is possible to generate conduction abnormalities in animals by pharmacological or surgical procedures, there are no model systems that exhibit heritable pathology.

Atrial natriuretic factor (ANF), a peptide hormone that is synthesized and stored in the cardiac atria, is a major participant in the systemic regulation of extracellular fluid volume and electrolytes. Secretion of ANF into the blood stream elicits physiological responses, such as natriuresis and a concomitant decrease in blood pressure (*1*). The high abundance of ANF in the atria has facilitated the molecular cloning of ANF complementary DNA's, and subsequently genomic clones (*2*). The ANF gene is highly conserved between species and is divided between three exons and two introns.

The technique of introducing genes into the germ line of mice permits the simultaneous functional analysis of promoter sequences in every cell type of a given animal (*3–5*). The sequences required for the transcriptional regulation of the ANF gene in vivo were identified as follows: transgenic mice that carry fusions between the putative ANF promoter and the SV40 large T antigen oncogene (ANF-TAG) were generated. The fusion gene carried the segment at −500 to +77 bp relative to the ANF messenger RNA cap site, and a 2.7-kbp restriction fragment encompassing the SV40 early region. Orientation was such that transcripts originating from the ANF promoter would encode the oncoprotein. The fusion gene was microinjected into embryos, and transgenic mice were generated and screened (*6*). Eight ANF-TAG transgenic mice (Table 1) were subdivided into two groups on the basis of their relative longevity. The ANF-TAG's 24, 25, 52, 84, and 210 each survived long enough to generate progeny litters of mice, and in four out of five instances have transmitted their respective transgenes. In each case, the founder mouse survived at least 22 weeks before it died as a consequence of transgene expression. Conversely, ANF-TAG's 49, 54, and 75 died shortly after birth and hence no lineages could be established.

Atrial expression of the ANF-TAG fusion gene was demonstrated by Western blot analyses (Fig. 1A). An approximately 90-kD polypeptide that comigrates with COS-1–derived SV40 T antigen is present in the atria from an ANF-TAG 210 mouse, but not in nontransgenic atria. Similar results were obtained with the other ANF-TAG transgenic lines. Western blot analyses were performed to ascertain the fidelity of the

Cold Spring Harbor Laboratory, Cold Spring Harbor, NY 11724.

transgene ANF promoter (Fig. 1B). While T antigen was readily detected in the transgenic atria, expression of the fusion gene was not observed in the other tissues tested. Thus 500 bp of 5′ flanking sequence is sufficient to direct atrial-specific expression of the human ANF gene. Low levels of transgene expression in cell types that constitute a small fraction of the total number of cells in any of these tissues cannot be ruled out by these analyses. Indeed, low levels of ANF expression have been observed in the ventricle, lung, and various portions of the brain (*7*). However, the predicted fusion gene expression in these tissues, based on that observed for the endogenous ANF gene, is appreciably below 1 percent of that for atrial expression, and as such is below the sensitivity afforded by this technique.

Atrial T antigen expression has been observed in all adult animals from the ANF-TAG 24, 52, 84, and 210 lineages (Table 1). In addition, T antigen expression was seen in both the atria and ventricles of mice ANF-TAG 49 and 75 (that is, in two of the three founders that died shortly after birth). Ventricular ANF expression is normally observed during development, but this expression ceases shortly after birth (*8*). Thus, T antigen expression in young transgenic ventricle is not surprising. However, the relation between developmental expression of ventricular ANF and neonatal viability is unknown.

Histological analysis of an 8-week-old ANF-TAG 52 mouse heart indicates that the left and right atria are of similar size and morphology, and at this age they are indistinguishable from those of nontransgenic animals (Fig. 2A). A similar section stained for the presence of T antigen indicates that virtually every atrial cardiocyte is expressing the fusion gene (Fig. 2B). This distribution is identical to that for the endogenous ANF gene product (*7, 9*). The highly branched trabecular architecture characteristic of normal atria is readily seen with higher magnification (Fig. 2C).

Similar analyses of a 20-week-old ANF-TAG 52 mouse reveals a pathological response to T antigen expression. The right atrium in this animal is grossly hyperplastic, and its size has increased an estimated 10- to 20-fold (Fig. 2D). However, the hyperplastic right atrium has retained its overall structural organization, as evidenced by a relatively normal (albeit enlarged) gross architecture and the absence of any obvious sites of focal outgrowth. The left atrium is of normal size (Fig. 2D). Immunohistochemical analyses indicate that T antigen is expressed in both the hyperplastic right atrium and the nonhyperplastic left atrium (Fig. 2E). Oncoprotein accumulation is similar in both atria by this analysis, although Western blot analyses indicate a slight increase in T antigen levels in the right atrium. A similar distribution for the endogenous ANF gene product has been reported (*10*). The ventricles are devoid of significant T antigen expression, thus confirming the earlier Western blot results. At this stage of pathology, scattered nuclei have become enlarged and irregularly shaped; however, the branched trabecular organization of the atrium is still evident (Fig. 2F).

Hyperplastic growth of the right atrium is eventually lethal to the affected mice. The right atrium of such animals undergo extensive hyperplasia (in this case, a 12-week-old ANF-TAG 210 mouse (Fig. 2G); its overall size is three to five times that of the entire heart from a normal mouse of the same age. Atrial tissue virtually surrounds the cardiac ventricles. Overall, this reflects a several hundredfold increase in right atrial mass. The ventricles of the heart appear relatively normal; there are no obvious signs of ventricular hypertrophy or dilation. Immunohistochemical analysis shows that both left and right atria are expressing T antigen, and once again the ventricles are not expressing the oncoprotein (Fig. 2H). At this stage of pathology, the atrial cardiocyte nuclei are grossly enlarged and misshapened, and the characteristic architecture of the cardiocyte syncytium has been disrupted (Fig. 2I).

The most striking feature of the pathology resulting from T antigen expression is the asymmetrical nature of atrial hyperplasia. Thus far, three of the four ANF-TAG transgenic lines (24, 52, and 210) have developed the asymmetry. Of the approximately 30 transgenic animals examined to date that exhibited atrial pathology at necropsy, the hyperplasia was invariably on the right side of the heart. Moreover, the pathology has been observed as far as two generations removed from the founder mouse. Tumors have not been observed at sites other than the cardiac atria. Although both atria express similar levels of T antigen, only the right atrium is subject to gross hyperplasia. The asymmetry may reflect the expression of requisite angiogenesis factors, autocrine loops, or other necessary tumor progression factors. Differential activity of any of these factors could render the right atrium respon-

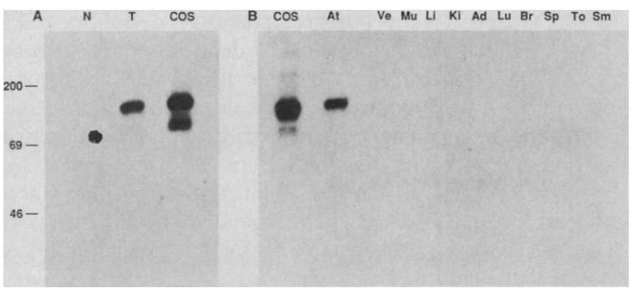

Fig. 1. Western blot analyses of T antigen expression in ANF-TAG transgenic mice. (**A**) Atrial expression of T antigen. Total atrial homogenate (500 μg) from nontransgenic (N) or transgenic (T) mice, and 50 μg of total protein homogenate from COS-1 cells were immunoprecipitated with monoclonal antibody to T antigen (pAB412) (17), displayed on 5 to 10 percent polyacrylamide gels, tranferred to GENESCREEN membrane, and probed first with rabbit antibody to T antigen and then with labeled goat antibody to rabbit immunoglobulin G (IgG). Western blots were performed essentially as described (*5, 18*). Molecular size standards (kilodaltons) were from Bio-Rad. The doublet seen for the COS marker was an artifact, and did not reappear on other gels with the same extract. (**B**) Tissue survey of fusion gene expression. Total protein homogenate (500 μg) from the indicated tissues were immunoprecipitated and processed for Western blot analyses as described above. At, atrial; Ve, ventricle; Mu, muscle; Li, liver; Ki, kidney; Ad, adrenal; Lu, lung; Br, brain; Sp, spleen, To, tongue; and Sm, submandibular gland.

Table 1. Status of ANF-TAG transgenic mice.

ANF-TAG lineage designation	Founder status*	Lineage established	Transgene copy number†	Atrial tag expression‡	Cardiac pathology§
24	S (38 W)	Yes	25	Yes	Yes
25	A (48 W)	Pending	2	ND	ND
52	D (24 W)	Yes	15	Yes	Yes
84	S (28 W)	Yes	30–40	Yes	No (25 W)
210	D (18 W)	Yes	20–30	Yes	Yes
49	D (1.5 W)	No	5–10	Yes	Yes
54	D (6 W)	No	15–20	ND	Yes
75	D (2.5 W)	No	ND	Yes	Yes

*Founder status: S, killed; A, alive; D, death as a consequence of atrial pathology. Numbers in parentheses refer to the age in weeks. †As estimated by comparative Southern blot analyses. ‡Expression was detected by Western blot analyses or immunohistochemistry; ND, not determined. §As evidenced at necropsy; ANF-TAG lines 24, 52, and 210 show gross asymmetrical atrial hyperplasia, while ANF-TAG numbers 49, 54, and 75 showed signs of both atrial and ventricular pathology.

sive and the left atrium refractile to T antigen. Indeed, there are many examples that implicate a link between the presence of autocrine growth factors and tumorigenesis (*11*).

The right atria are uniformly hyperplastic and retain a relatively normal anatomical appearance until the terminal stages of pathology. Such a condition is consistent with the idea that each right atrial myocardiocyte has the capacity to respond directly to T antigen, and does not require an additional activational event in order to exhibit hyperplasia. Similar patterns of hyperplasia have been observed in other systems of targeted oncogenesis as, for example, the bilateral hyperplasia of the Hardarian gland in MMTV–v-Ha-RAS transgenic mice and the gross thymic hyperplasia seen in GRF-T antigen transgenic mice (*12*). In the ANF-TAG mice, it is not clear if hyperplasia in the absence of malignancy reflects a natural refractility of atrial tissue against oncogenesis, or if it is a consequence of early death due to cardiac dysfunction. Thus, it is interesting that atrial tumors are rare in both humans and mice (*13*).

Electrocardiograph (ECG) analyses were performed on normal and ANF-TAG transgenic mice of various ages to assess the effect of atrial hyperplasia on the cardiac conduction system (*14*). Moreover, since the amplitude of ECG signals are theoretically proportional to tissue mass, this analysis could provide a simple noninvasive assay for the extent of atrial hyperplasia. Tail pulse traces were simultaneously recorded to show the relation between ECG signal and ventricular contraction. Experiments were performed on conscious animals to rule out potential artifacts due to anesthesia. ECG traces obtained from a 21-week-old nontransgenic F1 (C57B1/6J × DBA/2J) mouse shows typical P waves (atrial depolarizations) and QRS complexes (ventricular depolarizations); the amplitude of the P wave spike is much less than that of the QRS complex (Fig. 3A). There is a direct correlation between the appearance of the QRS complex and ventricular contraction spikes in the pulse trace (compare ECG and P traces in Fig. 3A). In the mouse, the signal corresponding to ventricular repolarization (the T wave) is obscured and difficult to detect (*15*). To the right is a survey photomicrograph of the heart used to generate the traces.

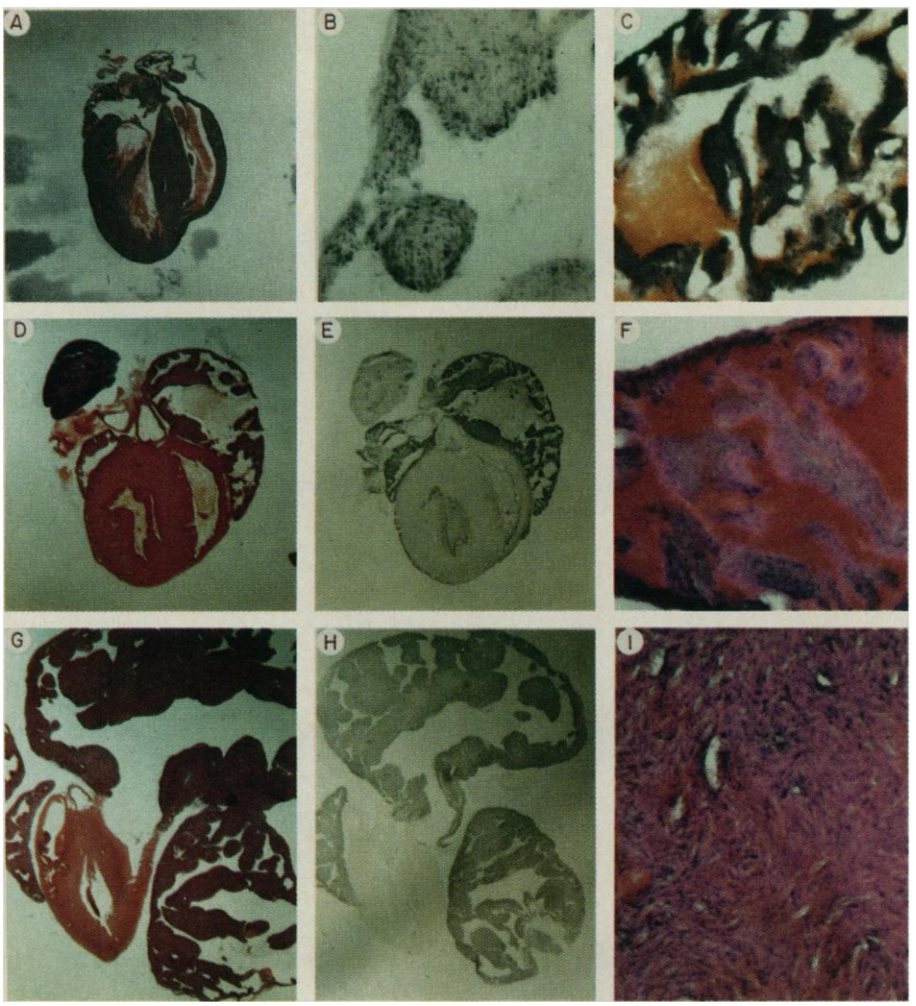

Fig. 2. Histological and immunohistological analysis of ANF-TAG transgenic mice. (A to C) Analysis of young ANF-TAG mice. (**A**) Survey photomicrograph of a heart section stained with hematoxylin and eosin (H and E). (**B**) Photomicrograph (×25) of the right atrium stained for the presence of T antigen. (**C**) Photomicrograph (×25) of the right atrial wall of a specimen stained with H and E. (D to F) Analysis of ANF-TAG mice with intermediate atrial hyperplasia. (**D**) Survey photomicrograph of a heart section stained with H and E. (**E**) Survey photomicrograph of an adjacent section stained for the presence of T antigen. (**F**) Photomicrograph (×25) of the right atrial wall stained with H and E. (G to I) Analysis of ANF-TAG mice with late stage hyperplasia. (**G**) Survey photomicrograph of a specimen stained with H and E. (**H**) An adjacent section stained for T antigen. (**I**) Photomicrograph (×25) of a section stained with H and E. For histological analyses, tissues were postfixed [in either 4% paraformaldehyde in 1× phosphate-buffered saline (PBS), or in acetone:methanol (1:1)], cryoprotected in 30% sucrose, sectioned at 10 μm, and stained with H and E. For immune histology, cryoprotected sections were reacted with rabbit antibody to T antigen, followed by a horseradish peroxidase–conjugated second antibody. The stain was generated by a diaminobenzidine reaction (*5*).

ECG and pulse rate traces from a young (8-week-old) ANF-TAG 52 mouse are indistinguishable from the nontransgenic control (Fig. 3B). The right atrium from this animal is normal in appearance and shows no signs of hyperplasia. However, the ECG and pulse rate traces generated by a 21-week-old ANF-TAG 52 mouse indicate a disruption of the conduction system (Fig. 3C). The ECG shows that the P waves are altered; both the duration as well as the relative amplitude of the P waves have increased. The QRS spikes are of normal shape and duration, and still dominate the trace (the identity of QRS spikes are confirmed by their relative alignment with contraction spikes in the pulse trace). Irregularities in the heart rate are present at the right end of the trace, and two P wave spikes are observed over the arrhythmic contraction cycles. The right atrium of the heart used to generate these traces is hyperplastic while the left atrium is relatively normal (Fig. 3C).

The ECG and pulse rate generated by a 30-week-old ANF-TAG 52 mouse reveals that the QRS complex no longer dominates the recording (Fig. 3D). In the regions of regular pulse, there are two spikes in the ECG trace for each contraction registered in the pulse rate trace, suggesting that the P waves are now present at an amplitude similar to that of the QRS complexes. Once again, multiple ECG spikes are present over the arrhythmic regions. Histological analyses indicate that the atrial pathology is of moderate severity. As atrial hyperplasia progresses, there is a corresponding increase in

the degree of conduction disruption (Fig. 3, E and F). The relative amplitudes of the ECG spikes vary in these traces, thus making it difficult to identify discrete P and QRS waves. Cardiac arrhythmias are apparent throughout the pulse traces of both animals. In both instances, atrial mass has exceeded that of the ventricles.

There is an apparent increase in heart rate (tachycardia) which accompanies atrial hyperplasia (690 to 730 beats per minute; see Fig. 3, C to F). However, this increase in heart rate is within the normal range of pulse rates reported for inbred mice [310 to 840 beats per minute (*16*)]. The tachycardia and arrhythmia may be due to the presence of ectopic pacemaker activities caused, for example, by ischemia resulting from the proliferation of atrial cardiocytes. Alternatively, the conduction abnormalities may result from a reentry phenomenon directly related to the large mass of the hyperplastic atria. With further characterization, these animals may prove to be a useful system to study cardiac conduction abnormalities. Moreover, the asymmetrical nature of atrial pathology makes these mice an attractive system in which to assess the events required to commit cells to the hyperplastic state.

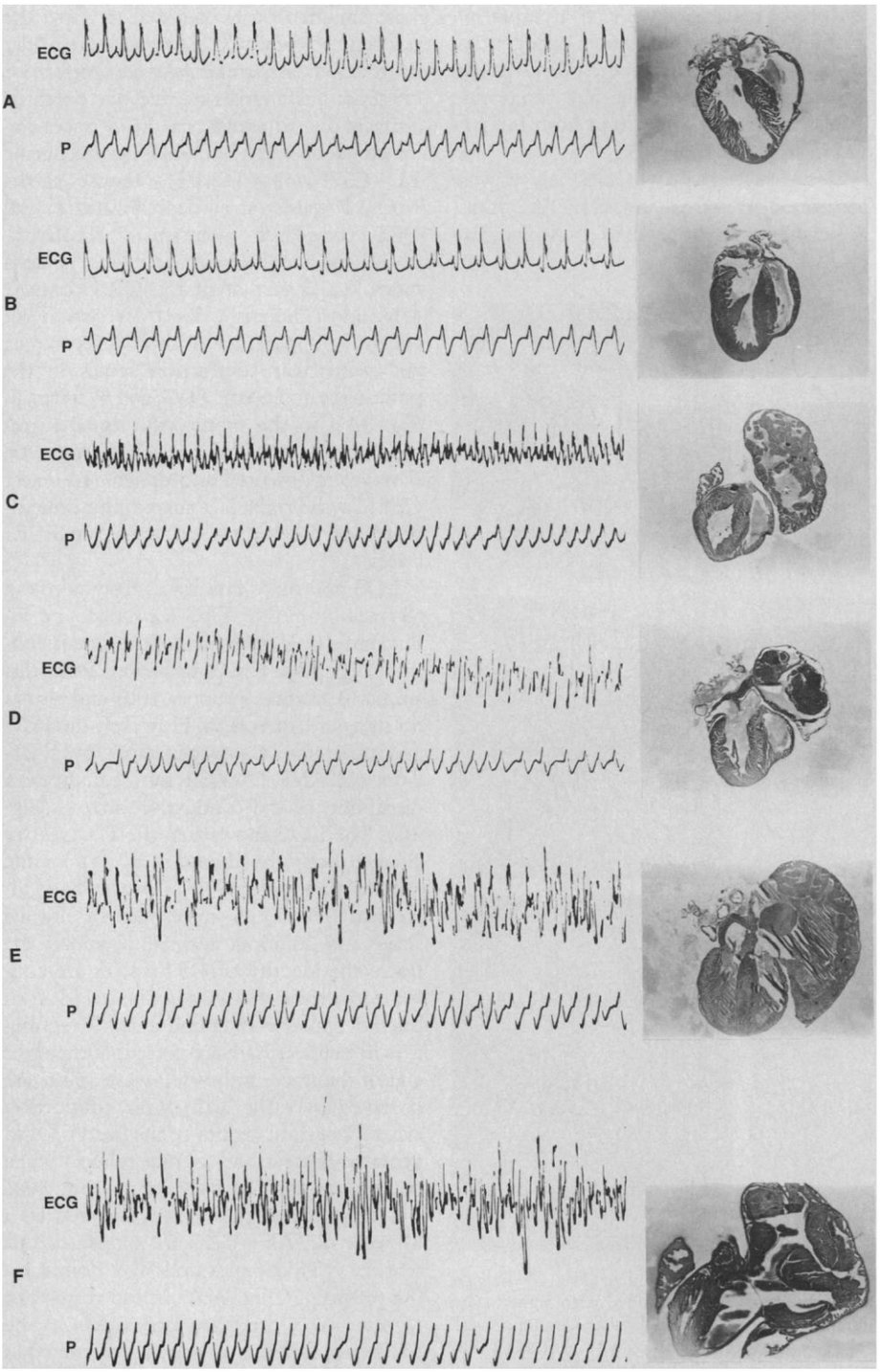

Fig. 3. ECG analysis of ANF-TAG mice. The ECG traces (labeled ECG) and pulse traces (labeled P) were recorded simultaneously on conscious animals with a Narco Biosystems Mark III physiograph interfaced with a high gain coupler. Electrodes were placed in the standard lead-1 position. Recordings were at a sensitivity of 20 mV/cm, a voltage gain of ×100, a time constant of 3.2 seconds, and a chart speed of 5 cm per second. Simultaneous pulse traces were recorded with a second channel interfaced with a Narco Biosystems pneumatic pulse transducer and a programmed electrosphygmomanometer. To the right of each set of traces is a survey photomicrograph of the heart used to generate the recording; the samples were processed as in Fig. 2. (**A**) A 21-week-old nontransgenic mouse. (**B** to **F**) ANF-TAG 52 mice that were 8, 21, 30, 26, and 28 weeks old, respectively.

REFERENCES AND NOTES

1. J. H. Laragh, *N. Engl. J. Med.* **313**, 1330 (1985); B. Leckie, *Nature (London)* **326**, 644 (1987); P. Needleman, *ibid.* **321**, 199 (1986).
2. S. Argentin *et al.*, *J. Biol. Chem.* **269**, 4568 (1985); C. E. Seidman, K. D. Block, K. A. Klein, J. A. Smith, J. G. Seidman, *Science* **226**, 1206 (1984); B. D. Greenberg, G. H. Bencen, J. J. Seilhamer, J. A. Lewicki, J. C. Fiddes, *Nature (London)* **312**, 656 (1984); M. Nemer *et al.*, *ibid.*, p. 654; M. Maki *et al.*, *ibid.*, **309**, 722 (1984); S. Okinawa *et al.*, *ibid.*, p. 724; C. E. Seidman *et al.*, *Science* **225**, 324 (1984); M. Yamanaka *et al.*, *Nature (London)* **309**, 719 (1984); R. A. Zivin *et al.*, *Proc. Natl. Acad. Sci. U.S.A.* **81**, 6325 (1984).
3. R. D. Palmiter and R. L. Brinster, *Cell* **41**, 343 (1985); *Annu. Rev. Genet.* **20**, 465 (1986).
4. R. L. Brinster *et al.*, *Cell* **37**, 367 (1984); F. Kelly, O. Kellerman, F. Mechali, J. Gaillard, C. Babinet, in *Cancer Cells,* M. Botchan, T. Grodzicker, P. A. Sharp, Eds. (Cold Spring Harbor Laboratory, 1986), vol. 4; K. A. Mahon *et al.*, *Science* **235**, 1622 (1987); D. M. Ornitz *et al.*, *Cold Spring Harbor Symp. Quant. Biol.* **50**, 411 (1985).
5. D. Hanahan, *Nature (London)* **315**, 115 (1985).
6. B. Hogan, F. Costantini, E. Lacy, *Manipulating the Mouse Embryo: A Laboratory Manual* (Cold Spring Harbor Laboratory, Cold Spring Harbor, NY, 1986).
7. K. D. Bloch, J. G. Seidman, J. D. Naftilian, J. T. Fallon, C. E. Seidman, *Cell* **47**, 695 (1986); D. G. Gardner *et al.*, *Proc. Natl. Acad. Sci. U.S.A.* **83**, 6697 (1986); C. B. Saper *et al.*, *Science* **227**, 1047 (1985); D. G. Gardner, G. P. Vlasuk, J. D. Baxter, J. C. Fiddes, J. A. Lweicki, *Proc. Natl. Acad. Sci. U.S.A.* **84**, 2175 (1987); R. C. Wiegand, M. L. Day, C. P. Rodi, D. Schwartz, P. Needleman, in *Atrial Hormones and Other Natriuretic Factors,* P. J. Mulrow and R. Schrier, Eds. (American Physiological Society, Washington, DC, 1987).
8. R. Zeller, K. D. Bloch, B. S. Williams, R. J. Arceci, C. E. Seidman, *Genes Dev.* **1**, 693 (1987).
9. C. Chapeau *et al.*, *J. Histochem. Cytochem.* **33**, 541 (1985).
10. I. Tanaka, K. S. Misono, T. Inagami, *Biochem. Biophys. Res. Commun.* **124**, 663 (1984); Y. Wei *et al.*, *J. Clin. Invest.* **79**, 1325 (1987).
11. A. B. Roberts *et al.*, *Proc. Natl. Acad. Sci. U.S.A.* **82**, 119 (1985); M. B. Sporn and A. B. Roberts, *Nature (London)* **313**, 745 (1985).
12. E. Sinn *et al.*, *Cell* **49**, 465 (1987); F. M. Botteri *et al.*, *Mol. Cell. Biol.***7**, 3178 (1987).
13. W. S. Colucci and E. Braunwald, in *Heart Disease,* E. Braunwald, Ed. (Saunders, Philadelphia, 1980); J. P. Strandberg and D. G. Goodman, in *The Mouse in Biomedical Research,* H. L. Foster, J. D. Snell, J. B. Fox, Eds. (Academic Press, New York, 1982).
14. A. C. Guyton, in *Basic Human Physiology,* A. C. Guyton, Ed. (Saunders, Philadelphia, 1971); G. H.

Mudge, *Manual of Electrocardiography* (Little, Brown, Boston, ed. 2, 1986).
15. A. G. Richards, E. Simonson, M. B. Visscher, *Am. J. Physiol.* **174**, 239 (1953).
16. D. A. Blizard and R. Welty, *J. Comp. Physiol. Psychol.* **77**, 337 (1971).
17. E. Harlow, L. V. Crawford, D. C. Pim, N. M. Williamson, *J. Virol.* **39**, 861 (1981).
18. H. Towbin, T. Staheleine, J. Gordon, *Proc. Natl. Acad. Sci. U.S.A.* **76**, 4350 (1979).
19. I thank R. Wiegand (Monsanto) for the human ANF gene and goat antibody to ANF; D. Hanahan (CSHL) for the SV40 early region clone; S. Alpert (CSHL) for the polyclonal antibody to T antigen; V. Dzau (Brigham's and Women's Hospital, Boston) and S. Grant (CSHL) for helpful suggestions; and W. Ryan (CSHL) for help in ECG interpretation. I thank D. Hanahan, W. Herr, W. Ryan, and T. Grodzicker for critical evaluation of the manuscript, and M. Ockler and D. Greene for help with the illustrations. Supported by grant HL 38605 (L.J.F.) and by a grant from Monsanto Company to CSHL This work is dedicated to the memory of Dr. Mark Diamond, State University of New York at Buffalo.

6 October 1987; accepted 21 January 1988

Modulation of Folding Pathways of Exported Proteins by the Leader Sequence

SOONHEE PARK,* GSEPING LIU, TRACI B. TOPPING, WILLIAM H. COVER,† LINDA L. RANDALL

Leader peptides that function to direct export of proteins through membranes have some common features but exhibit a remarkable sequence diversity. Thus there is some question whether leader peptides exert their function through conventional stereospecific protein-protein interaction. Here it is shown that the leader peptides retarded the folding of precursor maltose-binding protein and ribose-binding protein from *Escherichia coli*. This kinetic effect may be crucial in allowing precursors to enter the export pathway.

EFFICIENT TRANSFER OF PROTEINS through membranes during the processes of secretion and mitochondrial assembly in eukaryotes and of export in prokaryotes requires that the polypeptide has not adopted the stably folded structure of the mature species (*1, 2*). The current models for the export process incorporate the effects of protein conformation in different ways. One hypothesis prevalent among workers studying eukaryotic systems is that cells contain factors that actively unfold structured precursors by using the hydrolysis of nucleotide triphosphates as a source of energy (*3, 4*). A different notion, proposed for bacterial export, is that components within the cells bind to precursors before they fold into the final mature conformation and thereby maintain (or create) the export-competent state without having to disrupt established tertiary structure (*2, 5*). A defining and essential feature of a protein destined for export to the periplasm of *Escherichia coli* is that at its amino terminus it contains a leader sequence that is proteolytically removed to generate the mature species upon translocation across the membrane. Although functional leader peptides have some common features, there is no sequence similarity among such peptides. In bacteria the leader peptide is likely to be involved in several phases of export, initially in mediating entry into the export pathway, and subsequently in establishing interaction with the membrane at export sites (*6–8*). The precise role of the leader sequence in these separate steps may differ. Gierasch and co-workers (*9*) have suggested that during the encounter of the precursor with the membrane, the hydrophobicity and conformation of the leader are crucial for its proper insertion into the bilayer. We propose that, in addition, at an earlier step leader sequences allow the initial interaction with components of the export apparatus by modulating the folding pathways of precursor polypeptides, and we present evidence that the leader sequences of two periplasmic proteins from *Escherichia coli,* those of maltose-binding protein and ribose-binding protein, decrease the rates of folding of these proteins into their mature conformations.

Since we were interested in investigating the effect of leader sequences on the pathway of protein folding in the absence of interaction with any other cellular components, we purified the precursor and mature forms of the proteins (*10, 11*) and compared the kinetics of their folding in vitro. Both maltose-binding protein (molecular weight 38,500) and ribose-binding protein (molecular weight 29,000) are monomeric and contain no disulfide bonds. Maltose-binding protein contains eight tryptophanyl residues and thus the reversible unfolding-folding transition could be monitored by changes in the intrinsic fluorescence of tryptophan (*12*). In contrast, fluorescence spectroscopy could not be used to monitor the folding of ribose-binding protein, because that protein contains no tryptophan, and no change in the fluorescence of tyrosine was observed when the protein was denatured. Studies of the folding of ribose-binding protein were thus performed by measuring the resistance of the mature conformation to proteolytic degradation as the assay for folding.

Using fluorescence spectroscopy we have investigated the equilibrium, unfolding

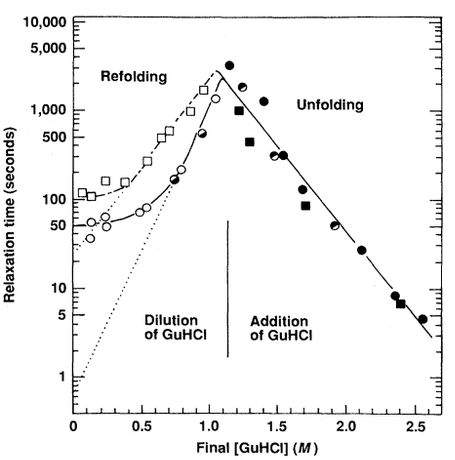

Fig. 1. Comparison of relaxation times for folding transitions of mature and precursor maltose-binding proteins. The relaxation times for folding (open symbols) and unfolding (closed symbols) transitions were obtained by monitoring the change in fluorescence of tryptophan. For unfolding transitions the protein was initially in 10 m*M* Hepes, *p*H 7.8, and guanidinium hydrochloride (GuHCl) was added to the final concentration shown. For refolding transitions, the protein was dissolved in 2*M* GuHCl, which was diluted to the final concentration shown. Fluorescence measurements were made with a Perkin-Elmer MPF-3L. The excitation and emission wavelengths used were 295 nm and 344 nm, respectively; mature maltose-binding protein (○); precursor maltose-binding protein (□). The precursor species was purified by a procedure that includes one cycle of unfolding-refolding (*10*). As a control, the mature species was subjected to a cycle of unfolding-refolding. Relaxation times determined with this material are represented by the half-closed circles; unfolding transition (◐); refolding (◑).

Biochemistry/Biophysics Program, Washington State University, Pullman, WA 99164.

*Present address: Genetic Engineering Center, Korea Advanced Institute of Science and Technology, Cheongryang 150, Seoul, Korea.
†Present address: Department of Biological Sciences, University of New Orleans, New Orleans, LA 70148.